Tribological properties of PTFE sealing materials with regard to bio-hybrid fuels

Marius Hofmeister[a], Alea Frische[a], Mathias Grunewald[b], Manuel Reddemann[b], Carolin Grütering[c], Lars M. Blank[c], Reinhold Kneer[b], Katharina Schmitz[a]

[a] RWTH Aachen University, Institute for Fluid Power Drives and Systems (ifas), Campus Boulevard 30, 52074 Aachen, Germany

[b] RWTH Aachen University, Lehrstuhl für Wärme- und Stoffübertragung (WSA), Augustinerbach 6, 52056 Aachen, Germany

[c] RWTH Aachen University, Institut für angewandte Mikrobiologie (iAMB), Worringer Weg 1, 52074 Aachen, Germany

Bio-hybrid fuels are carbon-neutral and can be produced based on sustainable raw material sources. Therefore, they represent a promising alternative to conventional fuels. However, the use of bio-hybrid fuels in automotive systems is challenging due to deviating fluid properties compared to conventional fuels. This applies especially to the compatibility of bio-hybrid fuels and sealing materials used in the automotive industry. One reliable way to prevent failure of seals is the use of PTFE materials, which, in turn, introduces new tribological challenges. For this reason, this contribution focuses on these challenges for radial shaft seals, which arise from the special characteristics of PTFE materials and bio-hybrid fuels.

1 Introduction

Bio-hybrid fuels are produced based on non-fossil carbon sources with renewable energy or by bio processes. Possible raw material sources are biomass from agricultural production, domestic wastes or wastes of the chemical industry. Therefore, bio-hybrid fuels are CO_2-neutral and represent a sustainable alternative to conventional fossil fuels with regard to climate change. A major advantage of bio-hybrid fuels over other energy carriers such as hydrogen or electricity is the easy implementation in existing vehicle systems and the use of existing infrastructure. This includes a worldwide network of petrol stations, suppliers and refinery plants.

The cluster of excellence "The Fuel Science Center" (FSC) is investigating bio-hybrid fuels with respect to their suitability as a substitute for conventional fuels like gasoline and diesel. In this context, methods for the prediction of fuel properties such as ignitibility indicators, spray behaviour or the tendency for sooth emission are developed. Using this methods, existing bio-hybrid fuels can be optimized or novel fuel candidates can be selected.

One prerequisite for the successful use of bio-hybrid fuels in automotive applications is the compatibility with existing sealing systems. However, many of the fuels studied within the FSC cause severe swelling as well as immediate failure of conventional sealing materials like NBR and FKM. This phenomenon particularly affects radial shaft seals in injection pumps. Preliminary examinations have already shown that

the only way to prevent swelling in this case is to use PTFE or PTFE compounds. For this reason, this contribution aims to investigate the tribological consequences stemming from the material properties of PTFE and bio-hybrid fuels.

The first part of the paper gives a brief overview over a few promising bio-hybrid fuel candidates investigated within the FSC. Both their chemical structure and typical fuel properties are addressed.

To illustrate the strong influence bio-hybrid fuels have on conventional sealing material, in the next part of the paper the results of an immersion test according to DIN ISO 1817 are presented. The test was conducted for the fuels described in the previous chapter and reference elastomers according to DIN ISO 13226.

Subsequently, several tribological values such as spreading coefficient and the penetrativity are determined. For this purpose, the used measurement set-up and the gathered results are presented. Furthermore, a test set-up for the determination of the wear behaviour of different combinations of PTFE materials and the considered bio-hybrid fuels is discussed.

Finally, the obtained results are discussed, and PTFE materials are evaluated regarding their usability as a sealing material for bio-hybrid fuels in automotive systems.

2 Bio-hybrid fuels

The investigated bio-hybrid fuels and their chemical structure are shown in Table 1. In addition to the bio-hybrid fuels, diesel and gasoline were also investigated to establish comparability with conventional fuels.

While diesel and gasoline consist exclusively of nonpolar hydrocarbons, it is noticeable that the fuels investigated also have polar components in the form of oxygen atoms in addition to nonpolar groups. The change in polarity can affect the behaviour toward sealing materials. For this reason, it cannot be assumed without further ado that the bio-hybrid fuels shown Table 1 are compatible with conventional sealing materials.

Table 1: Investigated bio-hybrid fuels

	Fuel	Chemical structure
Conventional fuels	Gasoline RON 95 (RON 95)	Various hydrocarbons
	Diesel EN 590 (D)	Various hydrocarbons
Bio-hybrid fuels	Mixture of methyl ketones (MK) n_C = e {11,13,15}	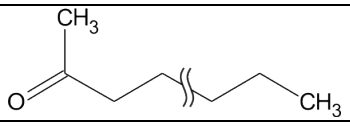
	Ethyl acetate (EA)	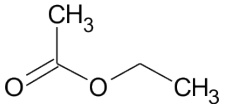
	1,3-Dioxolane (DIO)	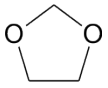
	Dimethoxymethane (DMM)	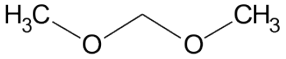
	Diethoxymethane (DEM)	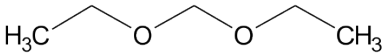

3 Material compatibility

In preliminary investigations the material compatibility of bio-hybrid fuels and sealing materials like NBR, FKM, VMQ and EPDM were investigated. For this reason, an immersion test according to DIN ISO 1817 was conducted [1]. In this context, the sealing materials were exposed to the investigated fuels. Over a period of 28 days, the parameters mass, volume and hardness are measured at defined intervals. Additionally, the discoloration of the fluid and the formation of particles were examined. As seal specimens, reference elastomers according to ISO 13226 are used [2].

In Figure 1 the results of the immersion test after 28 days are visible. On the x-axis the relative change of volume and on the y-axis the relative change of hardness are shown. Furthermore, tolerance areas for dynamic and static seals are marked in the diagram [3]. Each point in the diagram represents a combination of one sealing material and one of the bio-hybrid fuels mentioned before.

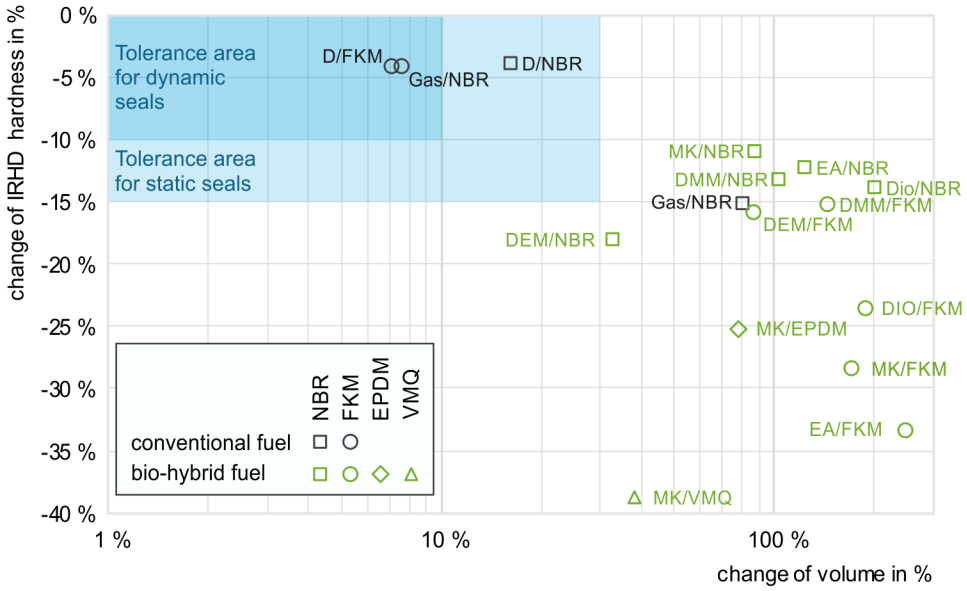

Figure 1: Change of volume and hardness for different conventional and bio-hybrid fuels

It can be seen that the conventional fuels diesel and gasoline lead to comparable low volume and hardness changes. The changes for FKM are within the tolerance range for both dynamic and static seals. The combination of NBR and diesel is within the tolerance are for static seals. Only for NBR combined with gasoline significantly larger changes of volume and hardness are visible. In contrast, all of the bio-hybrid fuels investigated lead to an extreme increase in volume and a sharp decrease in hardness, making it impossible to use them in technical systems. The greatest increase in volume has been observed for EA/FKM. The greatest decrease in hardness occurred for MK/VMQ.

The results of the immersion test illustrate that the investigated bio-hybrid fuels lead to extreme changes of material properties for conventional elastomer sealing materials. Therefore, an application in technical systems is not possible. To find suitable sealing materials which meet the requirements for seals in automotive systems, the immersion test was repeated for different composite materials and PTFE seals visible in Table 2. In contrast to the previous measurements, technical seals were used since the investigated materials are not available as reference materials.

Table 2: Investigated composite sealing materials

Material	Sealing type	Dimensions
PTFE/carbon	Radial shaft seal	25x38x7
PTFE	Flat material	2x20x25

For the seals shown in Table 2 no significant change of material properties could be detected. Neither, discoloration of the sample liquid and particle formation could be observed. For this reason, it can be assumed that the materials in Table 1 are chemically resistant to the investigated bio-hybrid fuels. However, the insertion test does not allow any statement about tribological properties. Therefore, different wetting parameter will be discussed in the following.

4 Wetting properties

For the estimation of the lubrication behaviour of the investigated bio-hybrid fuels in combination with PTFE sealing materials, different wetting properties were determined. In the following, the spreading coefficient and the penetrativity are discussed with regard to dynamic sealing systems.

4.1 Spreading coefficient

To achieve good lubrication between two solid surfaces and to prevent wear, the formation of a liquid film between these surfaces is required. Whether a liquid can spread on a surface mainly depends on the cohesive and adhesive forces acting on the liquid. In Figure 2 a liquid droplet and the corresponding interfacial energies are visible.

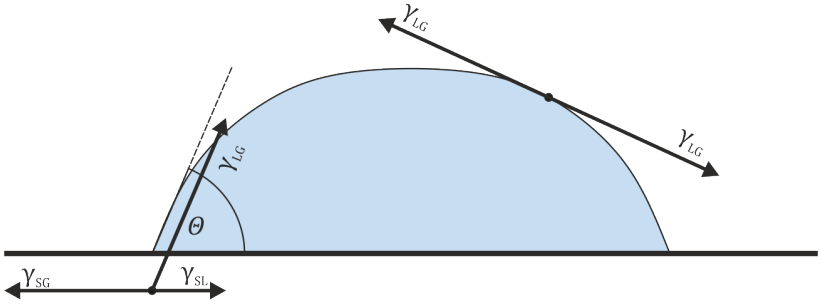

Figure 2: Droplet and acting surface energies

The work of adhesion W_A is composed of the interfacial energies γ_{SG}, γ_{LG} and γ_{SL}, as seen in equation (1), and aims to maximize the contact area between the droplet and the solid body. [4]

$$W_A = \gamma_{SG} - (\gamma_{LG} + \gamma_{SL}) \quad (1)$$

The cohesion work W_C counteracts the adhesion work W_A and aims to minimize the interface between the atmosphere and the droplet. The work of cohesion is given by equation (2) and is equal to twice the surface tension γ_{LG} of the liquid. [4]

$$W_C = 2 \cdot \gamma_{LG} \tag{2}$$

The spreading coefficient shown in equation (3) is the difference between the work of adhesion W_A and the work of cohesion W_C. [4]

$$S = W_A - W_C \tag{3}$$

In case $S > 0$, the adhesive work predominates, and complete wetting occurs. If S is smaller than 0, wetting is incomplete.[4]

In order to determine the spreading coefficient S in the further process, alternative representation methods are used for the work of adhesion. For example, authors Kaelble (4) and Wu (5) have established different calculation methods for W_A. [5, 6]

$$W_A = 2\left(\sqrt{\gamma_S^d} \cdot \sqrt{\gamma_L^d} + \sqrt{\gamma_S^p} \cdot \sqrt{\gamma_L^p}\right) \tag{4}$$

$$W_A = 2\left(\frac{2\gamma_S^d \cdot \gamma_L^d}{\gamma_S^d + \gamma_L^d} + \frac{2\gamma_S^p \cdot \gamma_S^p}{\gamma_S^p + \gamma_S^p}\right) \tag{5}$$

The symbols γ_S^d and γ_S^p represent the polar and disperse components of the interfacial tension of the solid body. The polar and disperse components of the liquid interfacial tension are indicated by γ_L^d and γ_L^p.

The method according to Kaelble is particularly suitable for liquids with a low surface tension. Since most of the investigated fuels have a low surface tension, in the following, the method of Kaelble is used for the determination of the work of adhesion [5].

4.2 Penetrativity

To ensure good lubrication in the contact between seal and shaft, the liquid must be able to penetrate the sealing gap. The penetrating fluid is primarily affected by viscous friction F_{vis} and surface tension F_{ST} as shown in Figure 3.

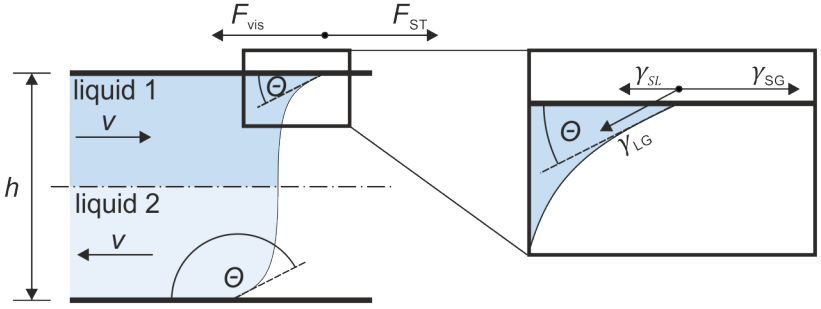

Figure 3: Penetration of a sealing gap

The viscous force is the product of the geometric dimensions of gap width W and gap length l as well as the viscosity η and shear rate $\frac{v}{2h}$ (6).[7]

$$F_{\mathrm{vis}} = \frac{v}{2h} \cdot \eta \cdot w \cdot l \tag{6}$$

The force F_{ST} caused by the surface forces corresponds to the difference of the interfacial energies γ_{SL} and γ_{LG}. According to Young and Dupre, the difference between σ_{SL} and σ_{SG} can be represented as the product of the cosine of the contact angle θ and the surface tension γ_{LG} of the liquid [8]. Taking the gap geometry into account, equation (7) is obtained.[7]

$$F_{\mathrm{ST}} = B \cdot \gamma_{\mathrm{LG}} \cdot \cos(\theta) \tag{7}$$

From equilibrium between the forces from (6) and (7), equation (8) follows. By rearranging, the penetrativity ψ is obtained, which is a measure of the ability of a liquid to penetrate a gap.[7]

$$\frac{2v}{h} \cdot \eta \cdot w \cdot l = \mathrm{w} \cdot \sigma_{\mathrm{LG}} \cos(\theta) \Leftrightarrow \frac{vl}{h} = \frac{\overbrace{\gamma_{\mathrm{LG}} \cos(\theta)}^{\psi}}{2\eta} \tag{8}$$

According to (8), high surface tension, low viscosity and a small contact angle lead to a high penetrativity, which improves lubrication in the gap. For contact angles greater than 90°, the liquid withdraws from the gap as shown in Figure 3 for liquid 2, which is not desirable.

If the surfaces of the gap are made of different materials, for the approximate calculation of the pentrativity, the formula from (9) can be used. Since the investigated sealing systems also consist of two different materials, for the evaluation of the penetrativity of the bio-hybrid fuels equation (9) is used.

$$\psi \approx \frac{\gamma_{\mathrm{LG}} \cos\left(\frac{\theta_1 + \theta_2}{2}\right)}{2\eta} \tag{9}$$

4.3 Determination of material properties

The wetting properties, spreading coefficient and penetrativity depends on both the material properties, like the liquid viscosity and surface tension, as well as on the surface energies of the solid materials. Thus, the measurement methods used for the determination of these parameter will be presented in the following.

4.3.1 Viscosity

For the determination of the kinematic viscosity, an Ubbelohde viscometer according to DIN 51562 is used [9]. The temperature of the sample liquid is controlled by a thermostat with a temperature accuracy of 0.01 K. To ensure accurate temperature control of the samples, the filled viscometers initially remain in the temperature control bath for 30 min. Subsequently, 7 measurements are conducted for each liquid.

The first two measurements are considered preliminary measurements and are not evaluated. The mean value is finally formed from the remaining 5 measurements.

Since the dynamic viscosity η is required for the calculation of the value penetrativity, the density ρ of the fluid is determined in addition to the kinematic viscosity ν. The dynamic viscosity can be calculated using equation (10).

$$\eta = \rho \cdot \nu \tag{10}$$

The measurement set-up for the determination of liquid density is shown in Figure 4. The set-up mainly consists of a displacement body and a precision tension scale. During the measurement process, the displacement body is immersed into the sample liquid and the resulting mass $m_{measured}$ is measured with the precision scale.

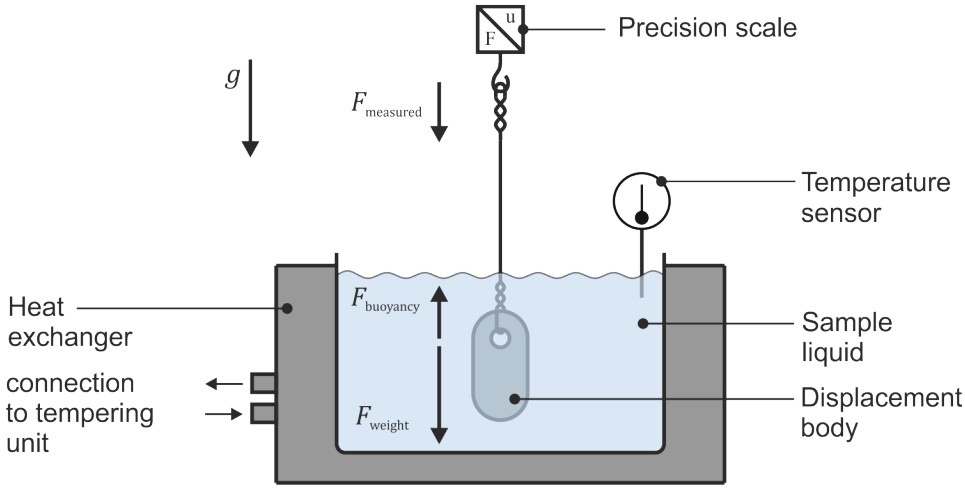

Figure 4: measurement set-up for the determination of liquid density

The measured mass $m_{measured}$ multiplied by the gravitation constant g equals the difference of the weight force and the buoyancy force (11).

$$m_{measured} \cdot g = \underbrace{m_{DB} \cdot g}_{weight\ force} - \underbrace{V_{DB} \cdot \rho_L \cdot g}_{buoyancy\ force} \tag{11}$$

By rearranging and shortening, one obtains equation (12).

$$\rho_L = \frac{m_{DB} - m_{measured}}{V_{DB}} \tag{12}$$

Since the volume V_{DB} and the mass m_{DB} of the displacement body are known, the liquid density can be calculated depending on the measured mass $m_{measured}$.

To control the temperature of the sample liquid, a heat exchanger is used, which is connected to temperature control unit with a temperature accuracy of 0.02 K.

The measurement was repeated 10 times for each liquid and temperature step.

4.3.2 Surface tension

The surface tension of the liquids is determined by means of the du Noüy ring method in accordance to DIN EN 14370 [10]. For the temperature control of the sample liquid a temperature control unit with a temperature accuracy of 0.02 K is used. In sum 5 measurements are performed for each sample liquid and each temperature step.

4.3.3 Interfacial tensions

The polar and disperse components of the solid materials are determined by means of the sessile drop method according to DIN 55660-2 [11]. For this purpose, drops of various reference liquids are placed on the investigated sealing materials with a manual microliter pipette. Subsequently, the contact angles of the droplets are recorded and evaluated with the methods specified by DIN°55660-2 [11]. Based on the contact angles, the polar and disperse interfacial tension were calculated according to the WORK method. The droplets were recorded with a Mitutoyo 3x magnification telecentric lens in combination with a Nikon digital SLR camera .The volume of each droplet is 2 µl. For each material 5 droplets are evaluated. The used reference liquids and their polar and disperse components are listed in Table 3.

Table 3: Reference materials for the determination of the polar and disperse interfacial tension [11]

Reference liquid/material	**Interfacial Tension** γ in mN/m	**Polar interfacial tension** γ^{p} in mN/m	**Disperse interfacial component** γ^{d} in mN/m
Water	72.8	51.0	21.8
1-bromo naphthalene	44.6	0	44.6
Ethylene glycol	47.7	16.8	30.9
Thiodiglycol	54.0	14.8	39.2
PTFE	19.0	0.5	18.5

For the determination of the polar and disperse components of the liquid interfacial tensions, the sessile droplet method is used, too. The procedure is the same as the one used to study the polar and disperse interfacial tension of the solid materials. For each sample liquid 10 droplets were evaluated. PTFE was used as reference material (Table 3).[12]

4.4 Results

The results for the physical fuel properties determined with the methods described in sections 4.3.1 and 4.3.2 are visible in Table 4. It can be seen that the viscosity of most bio-hybrid fuels is low and in the same order of magnitude as RON 95. Only the viscosity of the methyl ketone mixture with a value of 1.98 mPa·s is significantly

higher and comparable to that of diesel (1.83 mPa·s). The surface tension of all liquids is comparatively low, with values not exceeding 24.5 mN/m. The only exception is 1,3-dioxolane with a surface tension of 30.66 mN/m.

Table 4: Physical fuel properties at 40 °C

		Density in kg/m³	Kinematic viscosity in mm²/s	Dynamic viscosity in mPa·s	Surface tension in mN/m
Conventional fuels	**Diesel EN 590**	819,24	2,23	1,83	24,5
	RON 95	786,15	0,49	0,39	21,5
Bio-hybrid fuels	**MK**	812,79	2,43	1,98	24,5
	EA	876,08	0,42	0,37	21,73
	DIO	1041,54	0,50	0,50	30,66
	DMM	800,7	0,22	0,26	18,4
	DEM	809,72	0,41	0,33	19,1

With aid of the physical fuel properties from Table 4 and the measurement methods discussed in 4.3.3, the spreading coefficients (Figure 5) and the penetrativity (Figure 6) are determined.

The spreading coefficient for NBR and the conventional fuels diesel (5,52 mN/m) and gasoline (7,96 mN/m) is positive, which indicates complete wetting of the seal surfaces. The values for FKM in combination with diesel and gasoline are both negative and suggest incomplete wetting. Since both FKM and NBR are used as sealing materials for conventional fuels in automotive applications, the values for diesel and gasoline are to be understood as a reference for sufficient wetting.

Since the material compatibility between FKM and NBR is not given for bio-hybrid fuels, the values for the spreading coefficient are shaded here. They are to be understood as theoretical values, as technical implementation is not possible.

Furthermore the results in Figure 5 show that the spreading coefficient for all fuels in combination with PTFE and PTFE+C is much lower than for NBR and FKM in combination with conventional fuels. The lowest values are reached for 1,3-dioxolane (-37,46 mN/m for PTFE, -48,28 mN/m for PTFE+C). These results suggest that the surfaces of these seals can be wetted significantly worse than for NBR and FKM. The only exception is DMM. Positive values can be obtained for both PTFE (2,22 mN/m) and PTFE+C (2,83 mNm), which indicates complete wetting. The values obtained for steel differs significantly for each fuel and ranges from -10,13 mN/m for 1,3-dioxolane and 17,29 mN/m for DMM.

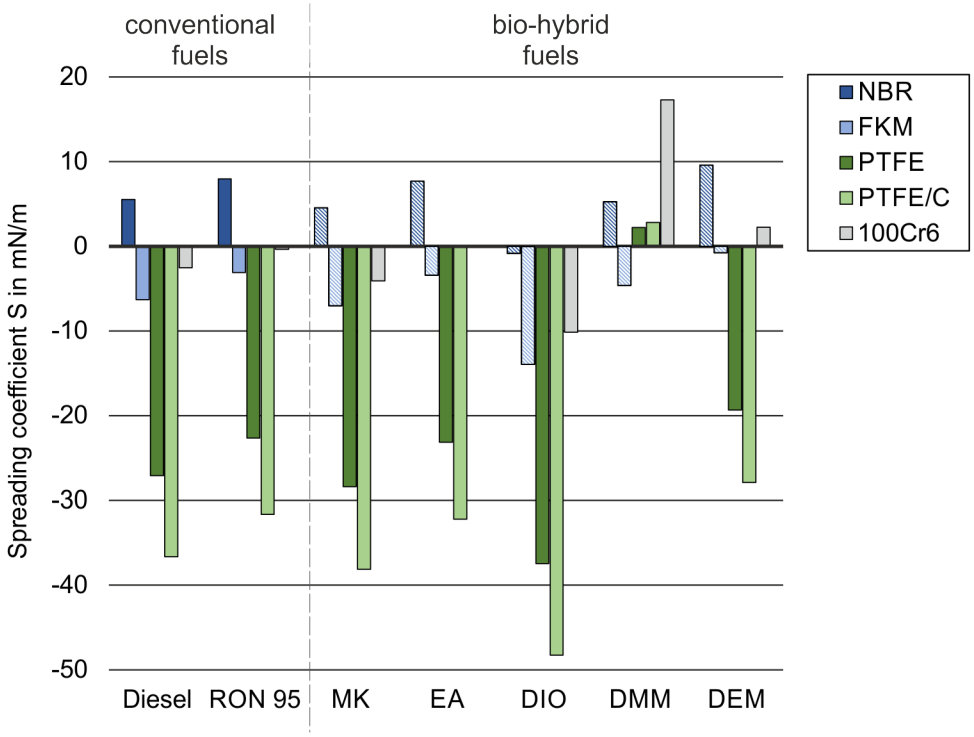

Figure 5: Spreading coefficient S at 40°C

The second wetting property that is determined, is the penetrativity. The results, shown in Figure 6, range from 1,05 to 14,3 m/s. Diesel and MK are located in a similar low range between 1,05 and 1,88. Average results are calculated for RON and DEM with values from 4,5 to 8. Values for EA and DIO are slightly higher, up to 8,8 or 10,5. The liquids seem to have a larger impact on the penetrativity than the solid materials. For this reason DMM is showing the highest penetrativity in a range from 8,7 to 14,3 m/s since it has the lowest dynamic viscosity of all investigated materials. Nonetheless there is a tendency that the combination of PTFE/100Cr6 is resulting in higher penetrativities, whereas FKM/100Cr is correlating with lower results. A good penetrativity in a shaft sealing system is expected for relatively high numbers. According to this EA, DIO and especially DMM are showing the most promising results, in particular in combination with a shaft sealing system made of PTFE and 100Cr6.

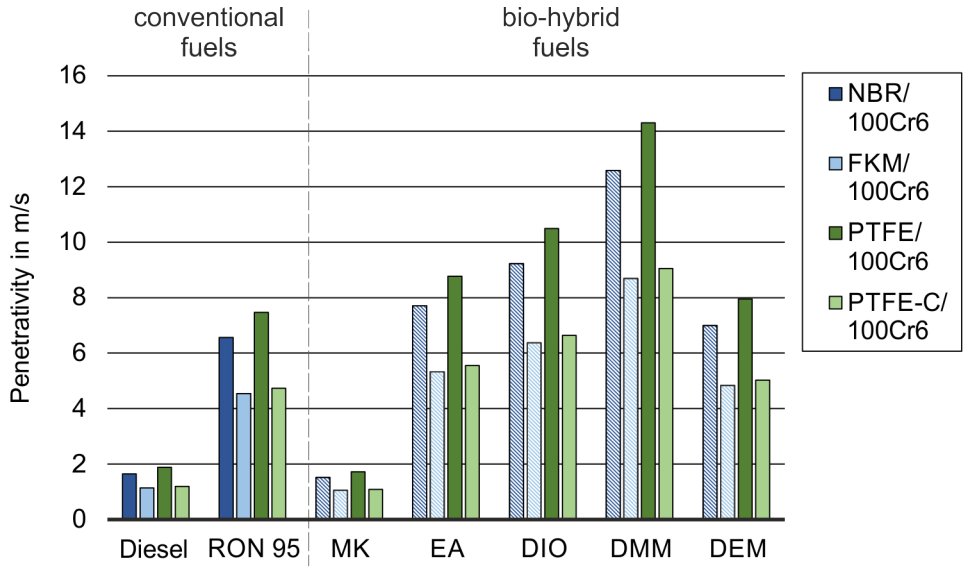

Figure 6: Penetrativity ψ at 40°C

5 Summary and Conclusion

This paper reviewed the poor material compatibility of conventional sealing materials used in the automotive industry and bio-hybrid fuels. For this purpose, an insertion test was carried out in accordance with DIN ISO 1817. The results have shown that PTFE materials exhibit good compatibility towards the bio-hybrid fuels investigated. Subsequently, basic principles for the determination of the spreading factor and penetrativity for PTFE, PTFE/C, NBR and FKM sealing material and bio-hybrid fuels were discussed and the measurement methods used were presented. According to the results most bio-hybrid fuels show bad spreading coefficient, while the penetrativity is comparable to conventional fuels or even better. One exception is DMM

According to the results, DMM shows the best wetting properties, in particular when it is combined with a PTFE sealing. A sealing, made of commonly used FKM elastomer, is not recommendable, whereas NBR, also a widely used elastomer, is showing acceptable wetting properties in combination with the regarded bio-hybrid fuels. The Penetrativity of PTFE is scoring the best results, if MK is excluded, but in regard of the spreading coefficient the results are poor, DMM not regarded. PTFE/C delivers consistently worse parameters in comparison to PTFE, again without regard of DMM. Noticeable are the relatively high penetrativities of DIO in contrast to the incomplete wetting of all tested elastomers.

6 Outlook

Since the determination of the "wetting properties" is only an initial estimate of the friction and wear behaviour of bio-hybrid fuels and PTFE-containing seals, further investigations will be carried out in the future to determine whether there is a correlation between "wetting properties" and wear or "friction".

In order to investigate the influence of the wetting properties determined in section 4 on wear and friction, a novel test set-up will be designed. The test set-up mainly consists of a driven shaft and a radial shaft sealing. During the measurement, the shaft sealing is exposed to the sample liquid and presses against the shaft. After each measurement process, seal and shaft are disassembled and investigated with regard to wear. A profilometer with a resolution in the sub-micrometer range shall be used for this purpose.

In the further course of the investigations, the presented bio-hybrid fuels will be examined by means of the mentioned test set-up. Due to the large number of possible bio-hybrid fuels, further wetting parameters and wear values are to be determined in the future. Once a sufficient number of fuels and seals have been examined, it will be checked whether an accurate prediction of wear can already be made on the basis of the wetting parameters.

7 Acknowledgements

Funded by the Deutsche Forschungsgemeinschaft (DFG, German Research Foundation) under Germany´s Excellence Strategy – Exzellenzcluster 2186 „The Fuel Science Center”.

8 Nomenclature

Variable	***Description***	***Unit***
F_{buoyancy}	Buoyancy force	[N]
F_{measured}	Measured force	[N]
F_{ST}	Force caused by surface tension	[N]
F_{vis}	Force caused by viscous friction	[N]
F_{weight}	Weight force	[N]
V_{DB}	Volume of the displacement body	[m^3]
W_{A}	Work of adhesion	[mN/m]
W_{C}	Work of cohesion	[mN/m]
m_{DB}	Mass of the displacement body	[m^3]
m_{measured}	Measured mass	[m^3]
$\gamma_{\mathrm{L}}^{\mathrm{d}}$	Disperse component of liquid interfacial energy	[mN/m]

γ_{LG}	Interfacial energy liquid - gas	[mN/m]
γ_L^p	Polar component of liquid interfacial energy	[mN/m]
γ_S^d	Disperse component of solid interfacial energy	[mN/m]
γ_{SG}	Interfacial energy solid - gas	[mN/m]
γ_{SL}	Interfacial energy solid - liquid	[mN/m]
γ_S^p	Polar component of solid interfacial energy	[mN/m]
ρ_L	Liquid density	[kg/m^3]
h	Height	[m]
S	Spreading coefficient	[mN/m]
g	Gravitation constant	[m^2/s]
l	Length	[m]
v	Velocity	[m/s]
w	Width	[m]
η	Dynamic viscosity	[mPa·s]
θ	Contact angle	[°]
ν	Kinematic viscosity	[mm^2/s]
ψ	Penetrativity	[m/s]

9 References

[1] Deutsches Institut für Normierung ev.: *DIN ISO 1817:2016-11 - Elastomere oder thermoplastische Elastomere – Bestimmung des Verhaltens gegenüber Flüssigkeiten,* Berlin: Beuth Verlag GmbH

[2] Deutsches Institut für Normierung ev.: *ISO 13226:2021-06 - Elastomere – Standard-Referenz-Elastomere (SREs) zur Charakterisierung des Verhaltens von Flüssigkeiten auf Elastomere,* Berlin: Beuth Verlag GmbH

[3] Richter, B.: *Bewertung von Beständigkeitstests von Elastomeren Werk-stoffen mit Getriebe- und Motorölen bezüglich des Funktionsverhalten von Radialwellendichtringen*, https://www.o-ring-prueflabor.de/de/fachaufsaetze/bewertung-von-bestaendigkeitstests-von-elastomeren-werkstoffen-mit-getriebe-und-motoroelen/, 2015

[4] Harkins, W. D.; Feldmann, A.: *Films. The Spreading of Liquids and the Spreading Coefficient*, In: J. Am. Chem. Soc., 1921, 44(12), pp. 2665-2685, doi:10.1021/ja01433a001

[5] Kaelble, D. H.: *Dispersion-Polar Surface Tension Properties of Organic Solids*, In: The Journal of Adhesion. 1970, 2(2), pp. 66–81, https://doi.org/10.1080/0021846708544582

[6] Wu, S.: *Polar and Nonpolar Interactions in Adhesion*, In: The Journal of Adhesion, 1973, 5(1), pp. 39–55, https://doi.org/10.1080/00218467308078437

[7] Washburn, E. W.: *The Dynamics of Capillary Flow*, In: Physical Review, 1921, 17(3), pp. 273–283, https://doi.org/10.1103/PhysRev.17.273

[8] Schrader, M. E., *Young-Dupre Revisited*, In: Langumir, 1995, 11(9), pp. 3585-3589, https://doi.org/10.1021/la00009a049

[9] Deutsches Institut für Normierung ev.: *DIN 51562-1:1999-01 – Messung der kinematischen Viskosität mit dem Ubbelohde-Viskosimeter,* Berlin: Beuth Verlag GmbH

[10] Deutsches Institut für Normierung ev.: *DIN EN 14370:2004-11 – Grenzflächenaktive Stoffe – Bestimmung der Oberflächenspannung,* Berlin: Beuth Verlag GmbH

[11] Deutsches Institut für Normierung ev.: *DIN 55660-2:2011-12 – Beschichtungsstoffe – Benetzbarkeit – Teil 2: Bestimmung der freien Oberflächenenergie fester Oberflächen durch Messung des Kontaktwinkels,* Berlin: Beuth Verlag GmbH

[12] Deutsches Institut für Normierung ev.: *DIN 55660-4:2012-04 – Beschichtungsstoffe - Benetzbarkeit - Teil 4: Bestimmung des polaren und dispersen Anteils der Oberflächenspannung von Flüssigkeiten aus einer Grenzflächenspannung,* Berlin: Beuth Verlag GmbH

10 Authors

RWTH Aachen University, Institute for Fluid Power Drives and Systems (ifas)
Campus Boulevard 30, 52074 Aachen, Germany:
Marius Hofmeister, M. Sc., marius.hofmeister@ifas.rwth-aachen.de
Alea Frische, alea.frische@ifas.rwth-aachen.de
Univ.-Prof. Dr.-Ing. Katharina Schmitz, katharina.schmitz@ ifas.rwth-aachen.de

RWTH Aachen University, Lehrstuhl für Wärme- und Stoffübertragung (WSA)
Augustinerbach 6, 52056 Aachen, Germany:
Mathias Grunewald, M. Sc., grunewald@wsa.rwth-aachen.de
Manuel Reddemann, reddemann@wsa.rwth-aachen.de
Univ.-Prof. Dr.-Ing. Reinhold Kneer, kneer@wsa.rwth.aachen.de

RWTH Aachen University, Institut für angewandte Mikrobiologie (iAMB)
Worringer Weg 1, 52074 Aachen, Germany:
Carolin Grütering, M. Sc., carolin.gruetering@rwth-aachen.de
Univ.-Prof. Dr.-Ing. Lars M. Blank, lars.blank@rwth.aachen.de